

The Influence of Added Mass on Rock Block Uplift in Plunge Pools

Erik F.R. Bollaert

*Director, AquaVision Engineering, Chemin des Champs-Courbes 1, CH-1024 Ecublens, Switzerland.
Email: erik.bollaert@aquavision-eng.ch*

Matteo P.E.A. Federspiel

Matteo P.E.A. Federspiel, Laboratory of Hydraulic Constructions (LCH), Ecole Polytechnique Fédérale de Lausanne, EPFL, Station 18, CH-1015 Lausanne, Switzerland; now: Project Engineer, IM Maggia Engineering SA, CH-6601 Locarno, Switzerland, Email: matteo.federspiel@im-maggia.ch

Anton J. Schleiss

Professor and Director, Laboratory of Hydraulic Constructions (LCH), Ecole Polytechnique Fédérale de Lausanne, EPFL, Station 18, CH-1015 Lausanne, Switzerland. E-mail: anton.schleiss@epfl.ch

ABSTRACT: This paper presents the influence of added mass, stiffness and damping on vibrational movements of rock blocks in plunge pools impacted by high-velocity jets. Turbulent flows impacting a pool generate severe pressure fluctuations at the water-rock interface. These pressures are transmitted through the joints of the rock foundation. Hence, during significant pressure differentials over and under a single rock block, the block may start vibrating or even be ejected from the surrounding mass. Large-scale laboratory measurements performed at the Laboratory of Hydraulic Constructions of the Swiss Federal Institute of Technology in Lausanne, Switzerland, allowed simultaneous measurements of pressure fluctuations and detailed vibrational movements and displacements of an artificial rock block. The 3D cubical shaped steel-made laboratory block has a side length of 200 mm and contains a large number of pressure transducers and displacement sensors. The circular shaped laboratory jet has an outlet diameter of 72 mm generating impact velocities of up to 30 m/s, i.e. at near-prototype scale. Turbulent pressure fluctuations and rock block displacements have been recorded simultaneously and at high frequencies. Sound comparison of these measurements with the equation of motion for a one-degree of freedom, spring-supported and damped rigid body vibrating in a still fluid, allow detailed assessment of the block movements. As such, for a wide range of jet impact velocities, plunge pool depths and jet impact positions, the added mass of the fluid during block movement as well as the stiffness and damping generated by the fluid are being determined. The paper presents a detailed comparison of measured and computed block vibrational movements for a single test run involving a jet impacting one of the vertical sides of the block. Sound calibration of the block vibration equation needed the introduction of significant added mass and viscous damping forces. Also, stiffness of the system was adapted to correctly reproduce the natural frequency of the block. As a conclusion, for one single test case, vibrational movements of a rock block impacted by a high-velocity turbulent flow have been assessed and described by a sound mathematical equation, including effects of added mass, stiffness and viscous fluid damping.

KEY WORDS: Added mass, Rock block uplift, Vibration, Stiffness, Damping, Pressure fluctuations.

1 INTRODUCTION

A large-scale experimental facility has been built at the Laboratory of Hydraulic Constructions (LCH) of the Ecole Polytechnique Fédérale de Lausanne (EPFL). The facility reproduces high-velocity plunging water jets that generate turbulent pressure fluctuations at the pool bottom and inside underlying artificial rock joints (Bollaert, 2002). The main finding obtained by the experimental facility is the presence and potential amplification of pressure transients inside closed-end and open-end rock joints. This amplification is due to the two-phase character of the air-water mixture inside the joints, which allows pressure wave reflection, amplification and even resonance. The pressure fluctuations inside the simulated rock joints are caused by the pressure excitation of the jet at the joint entrance. This excitation

depends not only on the form of the plunge pool and the associated macro-turbulent flow pattern, but also on the rock joint geometry.

The first series of rock joints tested were of simple shape, i.e. 1-dimensional or simplified 2-dimensional geometries. Real rock joints, however, have a much more complex geometry and are often interconnected (3-dimensional configuration). Hence, a second series of tests has been performed using an artificial 3D rock block separated from the surrounding rock mass by a network of fissures (Federspiel, 2011). The present paper analyzes the block vibrational movements for a single experiment involving a high-velocity jet.

2 EXPERIMENTAL FACILITY AND DATA ACQUISITION

2.1 Experimental Facility

A 300 mm diameter water supply conduit with a cylindrical-shaped jet outlet models the free falling jet (Figure 1). Due to constructive limitations, the supply conduit has a 90° bend just upstream of the jet outlet system. The end of the water supply conduit has been equipped with a 72 mm diameter (internal) cylindrical nozzle.

The plunge pool is simulated by a 3 m diameter cylindrical basin in steel reinforced Plexiglas with a height of 1.4 m. The maximum distance between the nozzle outlet and the plunge pool bottom is 1.0 m. The bottom of the basin is made of a rigid steel frame, covered by a 10 mm opaque Plexiglas plate. Inside the basin, two rectangular boxes (overflow boxes) made of opaque Plexiglas adjust the water level by a flat plate that is inserted. A restitution system consisting of four conduits of 220 mm diameter simulates the downstream conditions. These conduits are connected to the overflow boxes and conduct the water into the main reservoir of the laboratory (volume: 800 m³). The 63 m head pump is situated in the main reservoir of the laboratory, from which the water is pumped into the supply conduit. After being transferred through the restitution conduits, the water returns to the main reservoir. A closed water circulation system is so obtained. The maximum discharge is 120 l/s, which corresponds to an average jet outlet velocity of about 30 m/s.

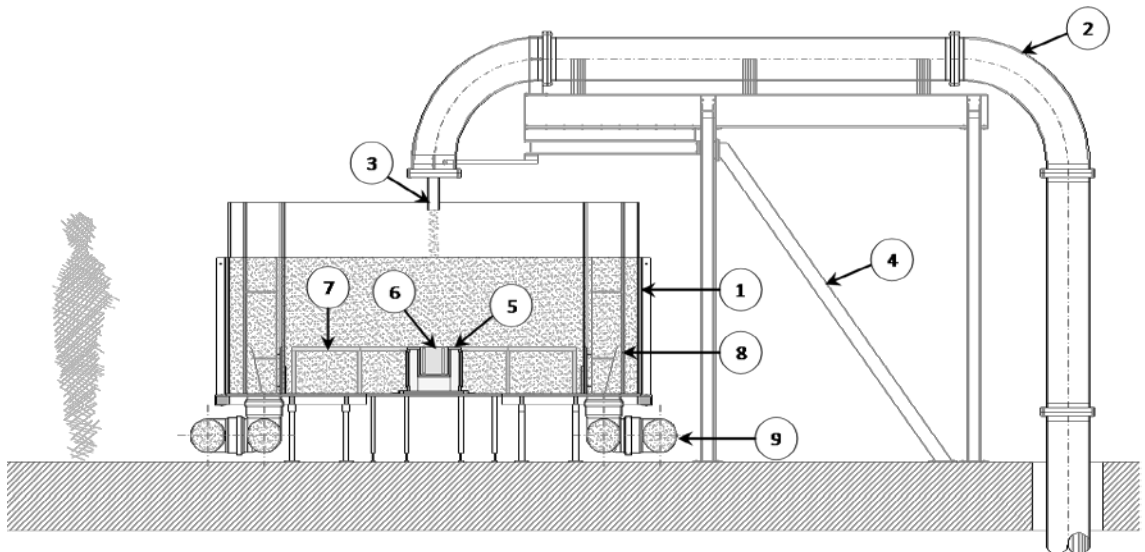


Figure 1 General view of the experimental facility (transversal section): (1) the plunge pool, (2) the water supply conduit, (3) the outlet nozzle, (4) the supporting steel structure, (5) the measurement box, (6) the highly instrumented block, (7) the new plunge pool bottom, (8) the overflow boxes and (9) the water restitution system.

The measurement box represents the rock foundation. It's a structure composed of steel plates (Figure 2). The dimensions are 402 mm of length, 402 mm of width and 340 mm of height. The thickness of the steel plates is 20 mm.

Inside this box, a large series of cavities allow to insert pressure and displacement transducers. All cavities are interconnected. To allow manipulation inside these cavities (i.e. modify the transducers position), all lateral walls have a 250 mm movable lid. The walls near the intelligent block are pre-perforated allowing to change the pressure transducers position. This allows to measure the water pressure generated by the jet inside the joints between the intelligent block and its surroundings, as well as to measure the corresponding displacement of the intelligent block. The box is impermeable to protect the electrical equipment.

In the center of the measurement box, a large cavity allows inserting the highly instrumented block. This intelligent block represents a single rock block in the rock mass with one degree of freedom (vertical movements). The cavity has a length of 202 mm, a width of 202 mm and a height of 201 mm. The block has a cubical shape with a side length of 200 mm. The width of the steel plates has been optimized to have a density similar to real rock ($2'400 - 2'500 \text{ kg/m}^3$). On the top of the intelligent block, some holes have been pre-perforated to fix the pressure transducers. Between the measurement box and the block, a 3-dimensional fissure of 1 mm width is so created.

In total, 95 different positions are available for pressure transducer insertion. For the displacement transducers, however, the positions are fixed. Inside the intelligent block, pressure transducers have been inserted to measure the pressure at the pool bottom under high-velocity jet impact. On the outside walls of the block, eight vertically oriented guide plates have been constructed. These guide plates (eight contact points with the measurement box) limit the degree of freedom of the block to vertical movements only.

Finally, both the measurement box and the intelligent block have been placed inside the 3 m diameter cylindrical basin which simulates the plunge pool (Figure 2 on the left).

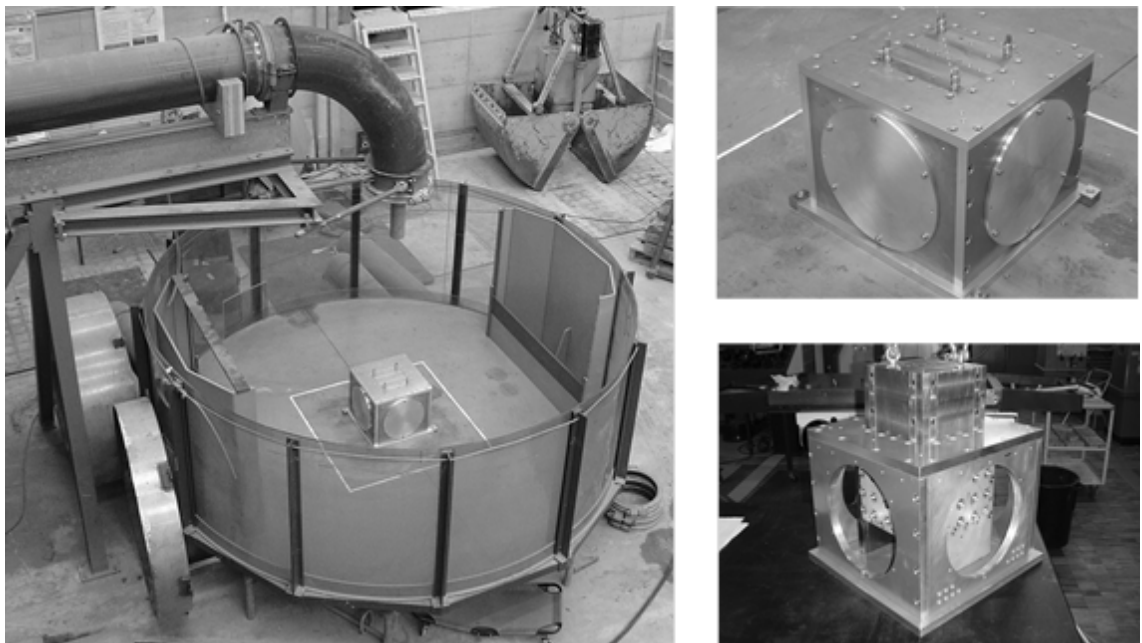


Figure 2 Left: The measurement box and the intelligent block insert into the cylindrical basin which simulates the plunge pool. Right bottom: the intelligent block is being inserted into the centre cavity of the measurement box. Right top: the intelligent block is now fully installed inside the measurement box.

2.2 Data Acquisition System

Data acquisition

The data acquisition system consists of a multifunction DAQ (Data Acquisition) device. The DAQ

device is a National Instruments (NI) card type USB-6259 series M. This device is a high-speed multifunctional data acquisition module optimized for superior accuracy at fast sampling rates. This DAQ device is characterized by 32 analog inputs SE (Single Ended) or 16 analog inputs DI (Differential) with a resolution of 16-bit and a maximal acquisition rate of 1,25 MSamples/second. The NI device is driven with author developed software running in the LabVIEW© environment.

Pressure transducers

A series of 12 KULITE HKM-350M-17-BAR-A micro pressure sensors are used for the pressure measurements. These sensors have a flush-mounted metal diaphragm with an absolute pressure range between 0 and 17 bars and a precision of ± 0.1 % of the full scale output. A solid state piezoresistive sensing element is located immediately behind this metal diaphragm and is protected by a metal screen. Force transfer is accomplished via an intervening film of non-compressible silicone oil. This sensing sub assembly is welded to a stainless steel body. The sensors have been developed to measure highly dynamic pressure phenomena, such as shock waves, and exhibit a very high resonance frequency (750 kHz).

Displacement transducers

Two BAUMER AG IWRM 18I9704/S14 displacement sensors are used for displacement measurements. These sensors are of the inductive type, with an absolute measurement range between 0 and 8 mm and a precision of less than 0.005 mm (static) or less than 0.01 mm (dynamic). Due to mounting constraints of the experimental facility the measurement range is only of 5 mm.

3 EXPERIMENTAL PARAMETERS

This paper analyzes the results obtained from a single test run involving asymmetrical jet impact on the artificial rock block. For this configuration, the plunge pool bottom is perfectly flat and the jet impact point in the plunge pool is centered along one of the block side faces - joint vertical axis (Figure 3). The plunge pool depth Y is of 0.60 m, for a diameter of the jet nozzle $D_j = 72$ mm. Hence, the Y/D ratio is of about 8.3, i.e. fully developed jet conditions.

The velocity of the impinging jet is an important parameter to modify the block and joint excitation (pressure field in the plunge pool and inside the 3-dimensional joint). Eleven different jet outlet velocities (between 2.5 m/s and 27.0 m/s or between 10 l/s to 110 l/s with 10 l/s steps) have been tested. Only the results for an outlet velocity of 27.0 m/s are discussed herein.

The 12 pressure transducers are mounted within the same vertical plane to reconstruct the pressure field around the block (Figure 3). Four transducers are installed inside the block and measure the pressure at the plunge pool bottom (309÷312): the first on the block center (309), the second at 25 mm, the third at 50 mm and the fourth at 75 mm from the block center. Four transducers are installed on one of the vertical walls of the measurement box (313÷317): the first at 50 mm from the plunge pool bottom and the following at 50 mm interval. Four transducers are situated underneath the block (318÷321): they have the same relative position as the four transducers that are installed inside the block (pressure at the plunge pool bottom).

The 2 displacement transducers (D1D and D2D, D2D is not visible on Figure 3) have a fixed position under the block in the measurement box.

For each water level and jet outlet velocity, three test runs have been performed. The data acquisition frequency is 1 kHz and the recording time of 65.5 seconds, providing $216 = 65 \cdot 536$ samples for each transducer. For each test run, about $983 \cdot 040$ samples are so being recorded (15 transducers: 12 pressure transducers, two displacement transducers)

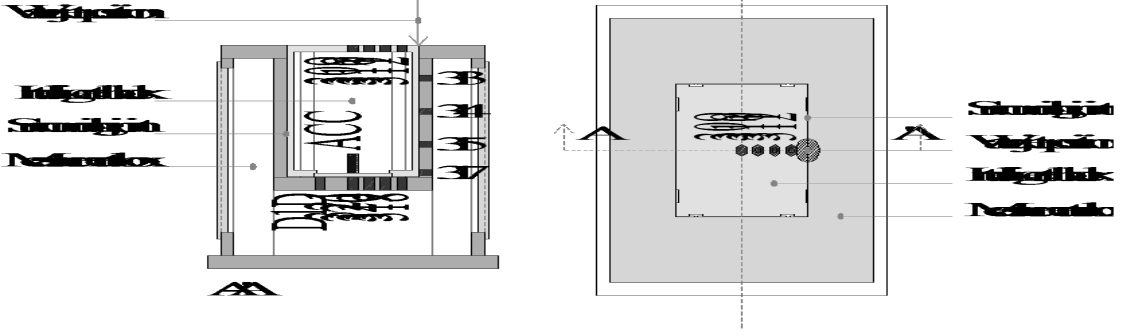


Figure 3 Left: Intelligent block transversal section with the transducers position. Right: jet impact and transducers position on the top of the intelligent block (at the plunge pool bottom).

4 EQUATION OF MOTION OF VIBRATING SUBMERGED BLOCK

The complex motion of a rock block submerged in a plunge pool that is subjected to the turbulent shear layer of an impacting jet is described here as a single-degree-of-freedom flow induced forced vibration of a submerged rigid body contained within the main rock mass. The corresponding equation of motion has a basic form similar to a typical mass-spring-dashpot system as follows (Figure 4):

$$(m_b + m_{add}) \cdot \ddot{x} + (c + c_{add}) \cdot \dot{x} + k \cdot x = F_{tot}(t) \quad (1)$$

where:

m_b	=	mass of the rock block	[kg]
m_{add}	=	added mass of the fluid surrounding the block	[kg]
c	=	viscous damping around the block	[kg/s]
c_{add}	=	added viscous damping around the block	[kg/s]
k	=	stiffness (spring constant) of the system during block displacement	[N/m]
x	=	absolute vertical displacement (uplift height) of the block	[m]
$F_{tot}(t)$	=	net total external force applied to the block as a function of time	[N]

The effective mass m_e of the system is obtained by superposing the mass of the block m_b and the mass of the surrounding fluid that must be accelerated during block acceleration m_{add} . The added mass force opposes the motion of the block. As such, the natural frequency f_n [Hz] of the system, for free vibrations without any forcing function, is written as follows:

$$f_n = \frac{1}{2\pi} \cdot \sqrt{\frac{k}{m_b + m_{add}}} \quad (2)$$

The total net force acting on the rock block at each time instant Δt is decomposed into pressure forces acting under and over the block, gravity forces, damping forces during block movement and finally a stiffness or spring force depending on the absolute block displacement. This system of equations is then solved numerically by applying a finite difference scheme and using the pressure forces over and under the block as measured for each time step by the pressure sensors on the physical model. Detailed comparison of the measured block displacements with the computed block displacements allows calibration of the following 3 parameters of eq. (1), the other parameters being either known or derived from the previous time step of the modeling process:

$\mu = c + c_{add}$	=	total viscous damping	[kg/s]
k	=	stiffness (spring constant) of the system	[N/m]
m_{add}	=	added mass of the fluid surrounding the block	[kg]

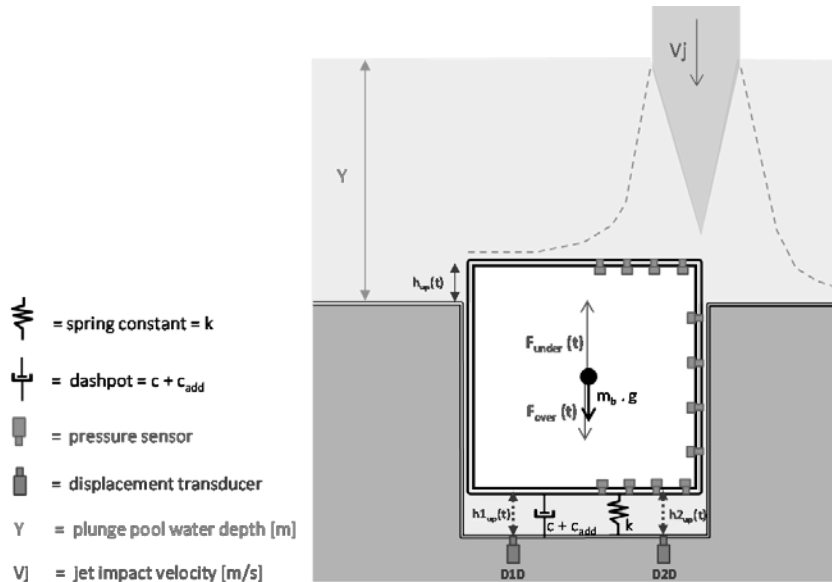


Figure 4 Main parameters of the single-degree-of-freedom mass-spring-dashpot system for block vibrations

5 NATURAL FREQUENCY, STIFFNESS AND DAMPING OF SUBMERGED BLOCK

The natural frequency of the submerged artificial rock block corresponds to the mode shape that characterizes its free oscillatory motion without damping effects. For a single degree-of-freedom oscillator, this frequency solely depends on the mass and the stiffness of the system.

The block natural frequency has been determined experimentally (Federspiel, 2011). To obtain this frequency, the block was inserted into the measurement box and excited by a hammer. Both the block and the measurement box have been excited by the hammer, with water inside the fissures and in the plunge pool. Spectral analysis of the measured frequencies show similar behavior for all test conditions, with a dominant frequency range between 5 and 9 Hz, for an average value of 7 Hz. According to Eq. (2), this corresponds to a ratio between stiffness k and mass m_b of the body between 990 and 3'200.

Second, the stiffness and damping of the system have been investigated by a series of tests. For the block being at rest inside the measurement box and the plunge pool filled with water, a 6 mm vertical displacement has been suddenly imposed to the block. During this movement, the pressures acting around the block have been recorded and analyzed. Next, the block has been suddenly moved down until its position at rest. The whole procedure has been repeated several times.

Figure 5a presents the pressures measured underneath the block during upwards movement, and Figure 5b the same pressures during downwards movement.

At start of block uplift (Figure 5a), the pressures between the block and the bottom suddenly decrease by about 1.5 bar in less than 0.05 sec. Initial values are recovered after about 0.2 additional seconds, the time necessary for the water to fill up and pressurize the gap formed between the block and the bottom. The flow of the displaced volume of water slightly reduces the pressure head underneath the block, however. A suction effect is thus generated during block upwards movements.

During downwards block movement (Figure 5b), the opposite phenomenon occurs, the pressures being increased during the movement by about 1 bar. When the block reaches the pool bottom, a severe pressure oscillation occurs. The compression of the water thus generates a force opposed to the block movement.

Hence, during small movements of a rock block contained in a 3D small fissure filled with water, significant forces that oppose the movements of the block are constantly being generated by the continuous change in fissure thickness and water flow in-and outside the fissure. These forces might be directly responsible for the stiffness and damping effects on the block movements as described by

equation (1) and as computed hereafter in § 6.

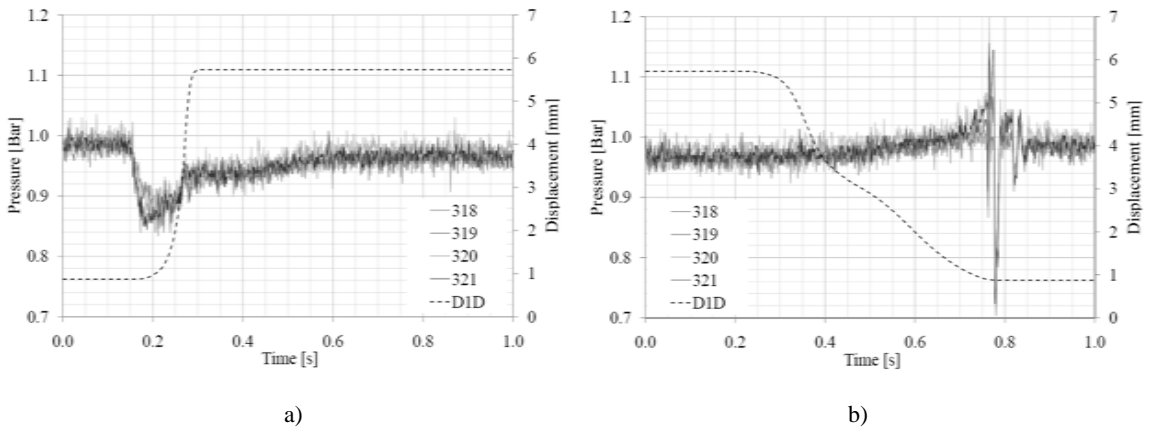


Figure 5 Measured block displacements (in [mm]) and corresponding pressures underneath the block for: a) suddenly imposed upwards movement; b) suddenly imposed downwards movement (Federspiel, 2011).

6 NUMERICAL MODELLING OF VIBRATING SUBMERGED BLOCK

The numerical modeling of the vibrational movements of an artificial rock block makes use of eq. (1). The results are illustrated in Figure 6 for a jet impact velocity of $V_j = 27.0$ m/s and a plunge pool water depth of $Y = 0.60$ m. As shown in Figure 4, the jet impacts the block asymmetrically, at the center of the vertical fissure separating the right hand side of the block from the measurement box. The pool depth of 0.60 m guarantees fully developed turbulent flow conditions, resulting in a highly aerated turbulent shear layer that generates pressure fluctuations over a large part of the surface area of the block.

First, Figure 6 shows the most convenient results obtained by optimization of a numerical modeling of block displacements without using added mass. Poor agreement is observed with the block displacements as measured by the displacement transducers D1D and D2D. The stiffness equals $10.0E6$ N/m and the viscous damping μ equals $4.0E4$ Ns/m. Extreme values computed occur much too frequently, and the frequency of the block displacements is clearly way too high, with an average computed value of 110 Hz. Also, relatively long periods of high respectively low displacements are completely disregarded by the computations.

Figure 7 compares the corresponding non-dimensional power spectral content of the measured and numerically computed block displacements, as well as of the measured net uplift pressures exerted by the turbulent jet on the block. Without accounting for added mass in the computations, the computed spectral content does not fit the measured one. The spectral content is, however, in very good agreement with the one of the net uplift pressures on the block, at least until frequencies of about 60 Hz.

Second, Figure 8 presents the corresponding results obtained by numerical modeling of block displacements with added mass included. By adding added mass up to about 100 times the block mass, good agreement can be obtained between computed and measured block displacements. The stiffness has been set at $1.7E6$ N/m and the viscous damping μ equals $2.8E5$ Ns/m during positive displacements and $5.0E5$ Ns/m during negative displacements. Extreme values computed are in agreement with the measured peaks and, accounting for added mass, the natural frequency of the block is now about 7 Hz. i.e. in excellent agreement with the natural frequency range of the system as experimentally determined in §5.

Also, the non-dimensional power spectral content of the numerically computed block displacements is now in good agreement with the measured spectral content. The dominant frequencies of the block vibrational displacements are situated between 1 and 5 Hz.

Finally, it has to be added that, by omitting added mass, viscous damping and stiffness all together, the computed block displacements indicate a rapid ejection of the block from its surroundings.

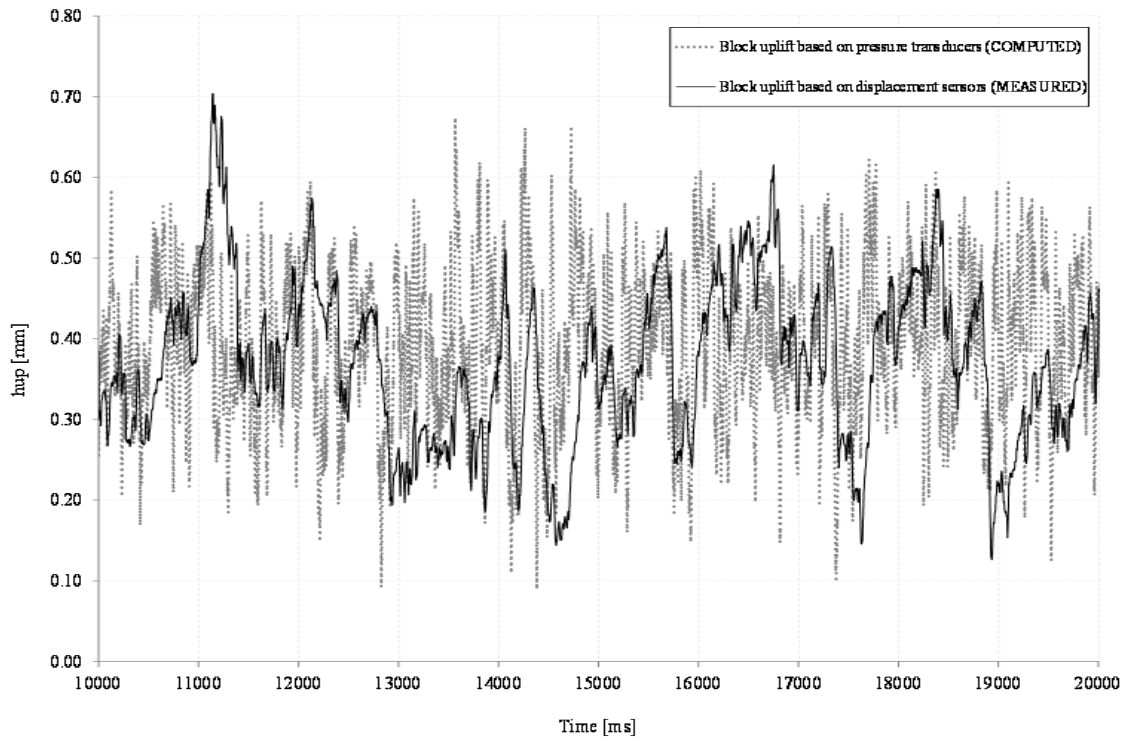


Figure 6 Comparison of measured and computed rock block displacements (in [mm]) for a jet impact velocity of 27 m/s and a plunge pool depth of 0.60 m. Computations WITHOUT added mass.

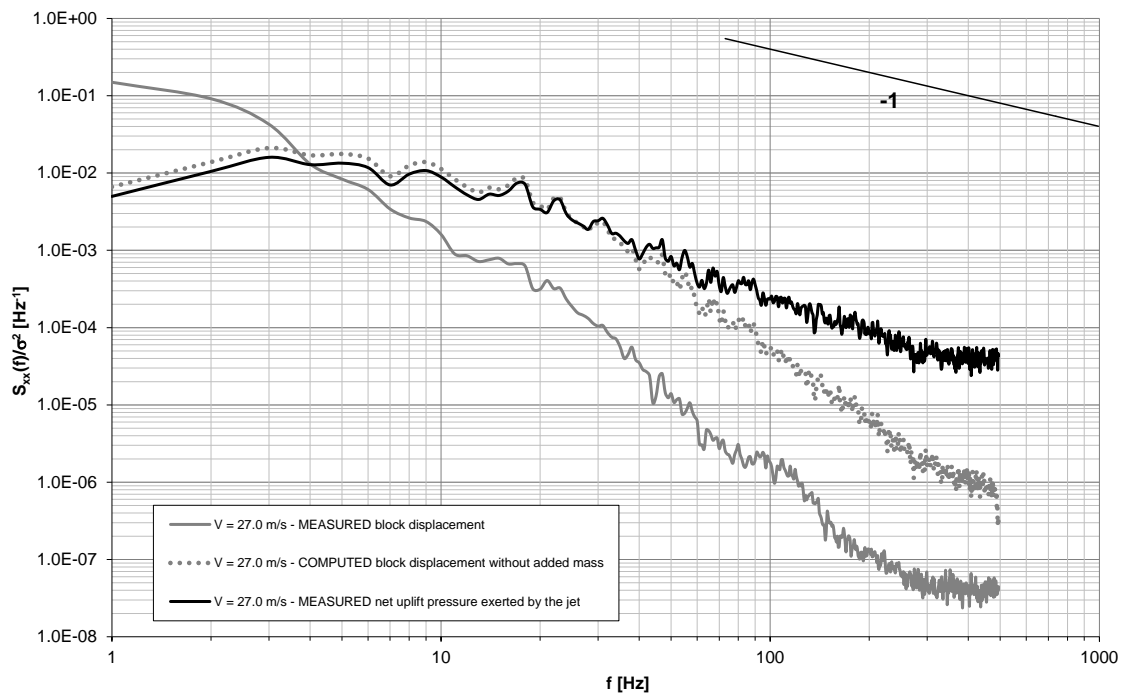


Figure 7 Non-dimensional power spectral content of measured and computed block uplift and of measured net uplift pressure exerted by the turbulent jet on the block. Computations WITHOUT added mass.

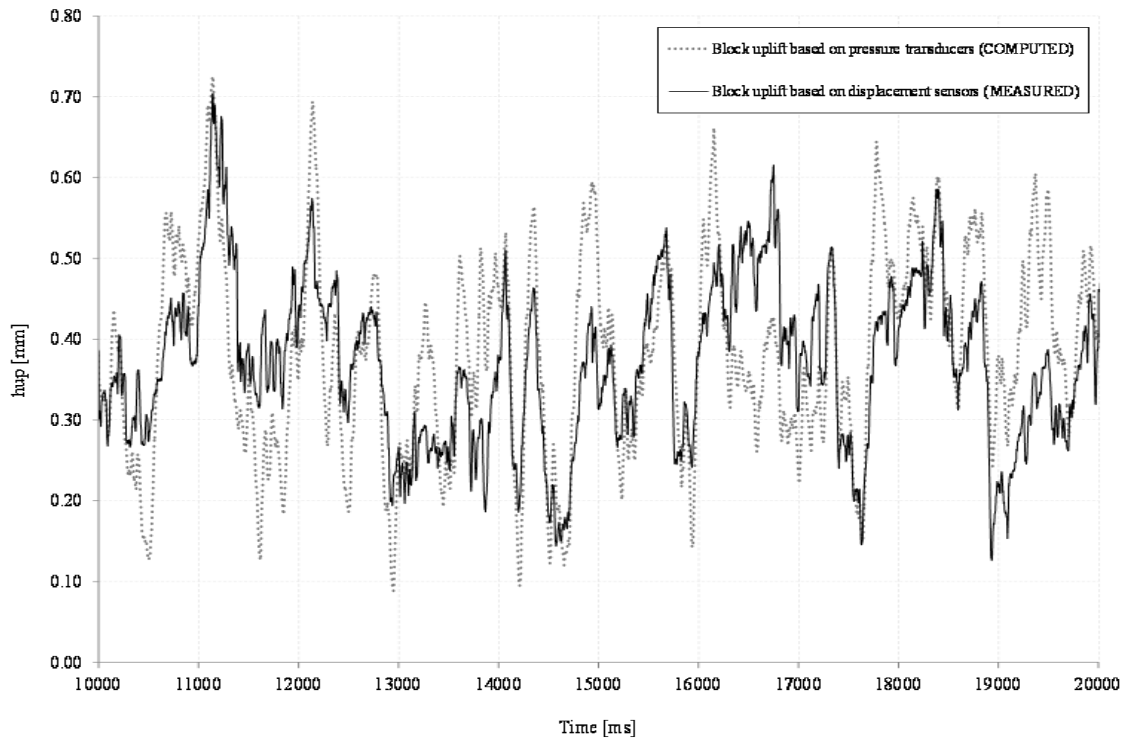


Figure 8 Comparison of measured and computed rock block displacements (in [mm]) for a jet impact velocity of 27 m/s and a plunge pool depth of 0.60 m. Computations WITH added mass.

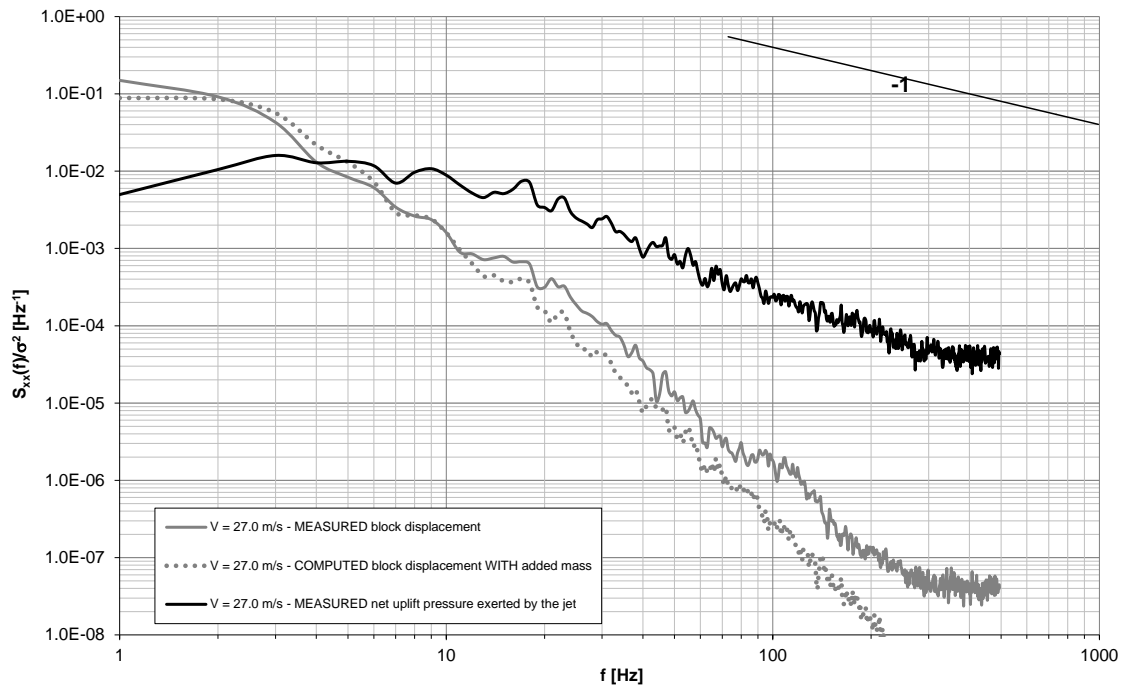


Figure 9 Non-dimensional power spectral content of measured and computed block uplift and of measured net uplift pressure exerted by the turbulent jet on the block. Computations WITH added mass.

7 CONCLUSIONS

This paper describes a test run with a near-prototype scaled experimental facility that generates high-velocity turbulent flows directly impacting an artificial cubic rock block. The 3D block is embedded in a plunge pool with 1mm fissures between the block and the surrounding rock mass. Analysis has been done of the pressure transients generated by the turbulent shear layer inside the fissures surrounding the block and of the simultaneous displacements of that same block. This has allowed computing the vibrational movements of the block by using the equations of a forced and flow-induced single-degree-of-freedom mass-spring-dashpot system.

Experimental investigation of the natural frequency of the submerged block by means of hammer blows has resulted in a low value of 5-9 Hz. Also, detailed high-frequency recordings of the pressures underneath the block during sudden (imposed) upwards or downwards movements of the block have shown the existence of significant forces that oppose against the movement of the block. These forces are related to the change in thickness of the fissure between the block and its surroundings, and to the flow of water in or out the fissure during block movements. As such, suction effects are generated during block uplift, and the opposite occurs during downwards movements.

As a result, sound calibration of the parameters of the equation of motion of the block needed the introduction of significant added mass as well as stiffness and viscous damping forces. For the high-velocity test described herein, the added mass revealed to be about 100 times the block mass. Moreover, the stiffness and viscous damping of the system were determined such that the measured block displacements are correctly reproduced by the computations in both the time and the spectral domain, as well as to respect the natural frequency of the block. This resulted in significant stiffness and damping.

In general, the block primarily reacts on the lower frequency part (< 10 Hz) of the pressure fluctuations generated by the impacting jet, especially in the range of 1-5 Hz. Higher frequencies seem to be of much less influence, reason for the significant damping introduced. Further investigations and numerical modelling for different positions of jet impact and different plunge pool depths, as well as for a range of jet impact velocities, are actually ongoing and aim at determining a sound generic mathematical formulation of block vibrational movements in a plunge pool impacted by high-velocity turbulent flow.

ACKNOWLEDGMENTS

The research work was supported by the Swiss National Science Foundation under contract SNF 200021-112620 & 200020-129606.

References

- Bollaert, E.F.R., 2002. Transient water pressures in joints and formation of rock scour due to high-velocity jet impact, Thèse N°2548 EPFL and Communication 13 of Laboratory of Hydraulic Constructions, Lausanne, Switzerland, ISSN 161-1179.
- Federspiel, M. P. E. A., Bollaert, E. F. R., and Schleiss, A. J. (2009). Response of an intelligent block to symmetrical core jet impact. In Proceedings of XXXIII IAHR Congress, Vancouver, Canada, pages 3573-3580. International Association for Hydro-Environment Engineering and Research (IAHR).
- Federspiel, M. P. E. A., Bollaert, E. F. R., and Schleiss, A. J. (2010). Experiments on the response of a rock block in a plunge pool loaded by a symmetrical jet impact. In Proceedings of 1st European IAHR Congress, Edinburgh, Scotland. International Association for Hydro-Environment Engineering and Research (IAHR).
- Federspiel, M.P.E.A., 2011. Response of an Embedded Block Impacted by High-Velocity Jets. Thèse N°5160 EPFL and Communication 47 of Laboratory of Hydraulic Constructions, Lausanne, Switzerland, ISSN 161-1179.
- Federspiel, M. P. E. A., Bollaert, E. F. R., and Schleiss, A. J. (2011). Dynamic response of a rock block in a plunge pool due to asymmetrical impact of a high-velocity jet. In Proceedings of XXXIV IAHR Congress, Brisbane, Australia. International Association for Hydro-Environment Engineering and Research (IAHR).